RESEARCH MEMORANDUM

SIMULATOR STUDIES OF THE ATTACK PHASE OF AN

AUTOMATICALLY CONTROLLED INTERCEPTOR

I - PRELIMINARY STUDIES OF THE LATERAL AND LONGITUDINAL

CONTROL SYSTEMS

By Albert A. Schy, Ordway B. Gates, Jr.,
and C. H. Woodling

II - SOME RESULTS OF A STUDY PERFORMED ON

THE TYPHOON COMPUTER

By Windsor L. Sherman and Leonard Sternfield

Langley Aeronautical Laboratory
Langley Field, Va.

NATIONAL ADVISORY COMMITTEE
FOR AERONAUTICS
WASHINGTON

August 18, 1955
Declassified May 16, 1958

NATIONAL ADVISORY COMMITTEE FOR AERONAUTICS

RESEARCH MEMORANDUM

SIMULATOR STUDIES OF THE ATTACK PHASE OF AN

AUTOMATICALLY CONTROLLED INTERCEPTOR

I – PRELIMINARY STUDIES OF THE LATERAL AND LONGITUDINAL

CONTROL SYSTEMS

By Albert A. Schy, Ordway B. Gates, Jr.,
and C. H. Woodling

II – SOME RESULTS OF A STUDY PERFORMED ON

THE TYPHOON COMPUTER

By Windsor L. Sherman and Leonard Sternfield

INTRODUCTION

The attack phase of the completely automatic interception of a bomber, which begins with lock-on of the interceptor radar and ends with firing of the interceptor armament, is at present receiving a great deal of attention. The initial phase of an analytical intestigation of several aspects of this problem has recently been completed at the Langley Aeronautical Laboratory. In this investigation the dynamics of an advanced-design interceptor, the geometry of the attack, and the guidance computer, which used first-order lead-collision guidance equations for rocket firing, were completely represented. Because of the detailed simulation of the problem, it was necessary to use a very large analog computer, and through the cooperation of the U. S. Navy, the Typhoon Computer at the U. S. Naval Air Development Center, Johnsville, Pa., was made available to the NACA for this investigation. Acknowledgement is made to the personnel of the Naval Air Development Center for their cooperation and assistance in setting up and operating the Typhoon Computer during this study.

Part I of this paper presents some results of preliminary studies of lateral and longitudinal control systems of the type used in the Typhoon investigation. In these studies appropriate simplifications were made to permit the use of the analog equipment available at the Langley Aeronautical Laboratory. In the following discussion, these studies are called the "simplified" studies, and the Typhoon study is called the "complete" study. In the simplified studies, three degrees of freedom were considered in both the lateral and longitudinal systems. Some results of the Typhoon investigation are presented in part II of this paper.

SYMBOLS

b   wing span

$$C_{l_\beta} = \frac{\partial C_l}{\partial \beta}$$

$$C_{l_p} = \frac{\partial C_l}{\partial \dfrac{pb}{2V}}$$

C_m pitching-moment coefficient

$$C_{n_\beta} = \frac{\partial C_n}{\partial \beta}$$

$$C_{n_p} = \frac{\partial C_n}{\partial \dfrac{pb}{2V}}$$

F_X, F_Y, F_Z aerodynamic forces along X-, Y-, and Z-axes, respectively

I_X, I_Y, I_Z moments of inertia about X-, Y-, and Z-axes, respectively

g   acceleration of gravity

Δg change in normal acceleration

K   constant

l_i, m_i, n_i direction cosines relating airplane principal body axes and
                  space axes

L'   rolling moment

M   Mach number

M_a predicted azimuth miss distance

M_e predicted elevation miss distance

m	airplane mass, W/g
M'	pitching moment
N	yawing moment
p	rolling velocity
q	pitching velocity
R_f	future range
r	yawing velocity
u_0	steady-state x-velocity
Δu	perturbation x-velocity
V	forward velocity
v	y-velocity component
W	airplane weight
w_0	steady-state z-velocity component
Δw	perturbation z-velocity component
α	angle of attack
β	angle of sideslip
γ	flight-path angle
$(\Delta\gamma)_D$	desired change in flight-path angle
δ_a	aileron angle
δ_e	elevator angle
δ_r	rudder angle
ϵ	resultant steering error, $\sqrt{\epsilon_a{}^2 + \epsilon_e{}^2}$
ϵ_a	azimuth steering error
ϵ_e	elevation steering error
ϵ_ϕ	roll-angle error

θ angle of pitch

ϕ angle of roll (or bank)

ψ angle of yaw

ω frequency

Subscripts:

c   command

cr   critical

i   1, 2, 3

o   steady-state conditions

One or two dots over a symbol indicates first or second time derivative, respectively.

I - PRELIMINARY STUDIES OF THE LATERAL AND LONGITUDINAL

CONTROL SYSTEMS

Figure 1 illustrates the tie-in system by which the input commands to the lateral and longitudinal control systems were obtained from outputs of the guidance computer. For a given orientation between the interceptor and the predicted target position, the elevation miss distance M_e, the azimuth miss distance M_a, the future range R_f, and the "time to go" t_g were obtained from the guidance computer. In order to compute the instantaneous miss distances, both the interceptor and the target were assumed to maintain their instantaneous velocities for the time t_g, at which time the rockets are fired. The rocket time of flight was 1.5 seconds, and the rocket velocity was parallel to the interceptor velocity at 2,000 feet per second. The miss distances were obtained in airplane coordinates. The input to the lateral (aileron) control system is the arc tangent of the ratio of azimuth and elevation miss distances. The lateral error disappears when the airplane rolls through the angle ϵ_ϕ, since the predicted target then lies in the longitudinal plane of the interceptor. The longitudinal error is the ratio of the elevation miss distance to the future range and is basically an error in flight path. This error commands an elevator deflection to aim the flight path toward the predicted target position. The rudder is used only to damp the lateral oscillation of the airplane and does not respond directly to the guidance commands. This simple tie-in system neglects the effect of gravity, and the resulting maneuver is therefore not properly coordinated. It was

desired to see whether a fast roll response would make the lack of
coordination unimportant.

A block diagram of the lateral control system is shown in figure 2.
In the simplified study a step command in bank (roll) angle was applied
and the airplane bank angle was fed back, as shown by the dotted line,
in order to obtain the bank error ϵ_ϕ. No target motions or guidance
were considered. In the complete study the bank error ϵ_ϕ was obtained
from filtered values of the miss distances calculated by the guidance
computer, without an actual bank feedback. The effect of the miss-
distance filtering on the bank command was largely eliminated in the
complete study by using cross-roll corrections in the filter; conse-
quently, no filter was included in the simplified analysis of the roll-
control system. The bank error was amplified and fed into the aileron
servo to obtain aileron deflections. Rate and acceleration feedbacks
were used to stabilize the airplane-servo loop. The transfer function
of the servo was represented by a first-order time lag, and the servo
was assumed to have limits on the magnitude and rate of its output
deflection.

Some characteristics of the airplane-servo system are now presented
to show the importance of various components in the lateral control system.
Figure 3 presents several inverse open-loop complex plots, showing some
undesirable properties of the interceptor as a roll-control system and
how these properties can be corrected. The imaginary part of the inverse
open-loop transfer function is plotted along the ordinate, and the real
part along the abscissa. Values of angular frequency ω are shown at
points along the curves. The curve labeled "airplane alone" represents
the simplest roll-control system, which would have simply the amplifier
and servo deflecting the aileron in response to the command. With servo
lags and limiting neglected, the response of such a system is determined
by the roll transfer function of the interceptor itself. Note that the
curve has a large loop, which indicates an undesirable dip in the fre-
quency response, and low values of the ordinate at high frequency, which
indicate insufficient roll damping. The undesirable loop in the curve
is caused by the Dutch-roll mode, as can be seen by comparison with the
curve in which a relatively strong yaw damper has been included in the
airplane transfer function to inhibit the Dutch-roll oscillation. The
third curve shows that by adding some roll-rate feedback, in addition to
the yaw damper, a desirable type of inverse open-loop curve is obtained.
Both the yaw damper and rate feedback were therefore included in the con-
trol system for the complete investigation.

The very strong effect of the Dutch-roll mode on the roll response
of this airplane is caused by the presence of a large product of inertia.
Although the product of inertia increases the Dutch-roll damping in the
present example, it also introduces a coupling between the yawing and
rolling which makes it very difficult to remove the Dutch-roll oscillation

from the rolling motion. It therefore appears that a large value of product of inertia is undesirable when a nonoscillatory roll response is required. The open-loop analysis is valid only for linear systems. However, since limits were put on the aileron and elevator rates and deflections, both the lateral and longitudinal control systems were actually nonlinear. Figure 4 presents some results showing typical effects of limiting on the lateral system. Time histories of roll response and aileron deflection are shown.

The aileron angle is limited to $\pm20^\circ$, and the rate of deflection is limited to $\pm120^\circ$ per second. The basic system had enough rate feedback to provide a well-damped response according to a linear analysis. As shown by the solid-line curves, the control-rate limiting causes a poor response with a neutrally stable oscillation. Although the addition of rate feedback tends to stabilize this oscillation, even a very large increase, which slows up the response considerably, leaves a slight amount of limiting oscillation, as can be seen from the dashed curves. The use of a small amount of acceleration feedback, however, eliminates the rate-limiting oscillation entirely. It can be seen that a smooth, rapid response is obtained with no limiting oscillation in the control. Acceleration feedback was therefore included in the complete study. It is interesting to note that a linear analysis shows that the combination of rate and acceleration feedbacks is also very effective in compensating for the destabilizing effect of a first-order time lag in the system. This result indicates that it may be possible to consider rate limiting in a control servo as being similar to an effective linear time lag in the servo. A more detailed analysis of the lateral system is presented in reference 1.

Figure 5 shows the longitudinal control system. In setting up the longitudinal attack problem, a simplified form of the first-order lead-collision guidance equations was used to calculate the longitudinal error input, which can be considered as an error in flight-path angle. This error was filtered and amplified, and, in some cases, also integrated, and the resulting signal was used to command a rate of change of flight-path angle $\dot\gamma$. Acceleration limiting was obtained by limiting this command in $\dot\gamma$. The limits used corresponded to 5g and -2g in the steady state. The error in $\dot\gamma$ was then amplified (and sometimes also integrated) and applied to the elevator servo which caused the airplane to maneuver. The integrator in the inner loop was sometimes used in order to make the steady output acceleration equal the command value. The use of this integrator was not essential, however, and good response could be obtained from the acceleration-command loop with or without this integrator by proper gain adjustment. The filter and servo dynamics were represented by first-order time lags, and the servo output was limited in rate and deflection. Pitch rate and acceleration feedbacks were found to be effective in stabilizing the airplane-servo loop, in a manner similar

to that already discussed in connection with roll rate and acceleration
feedbacks in the lateral system. Effects of speed loss were included in
the representation of the airplane response.

The interceptor was assumed to be flying at an altitude of 50,000 feet
at Mach number 2.2. The lock-on range was 60,000 feet, and at lock-on
the target was assumed to be above the interceptor and flying toward the
interceptor on a parallel path at Mach number 1.4. The radar lock-on
angles varied from 2^O to 10°, which corresponded to initial altitude dif-
ferences between 4,000 feet and 12,500 feet. Solutions were obtained
both for straight flying targets and for targets flying with constant
acceleration at lock-on. Against an accelerating target, the first-
order guidance requires that the interceptor accelerate in the steady
state. In order to obtain a steady acceleration with the control system
considered here, there must either be a steady-state bias-error input,
or the integrator must be used in the outer loop. If the tracking inte-
grator is not used, relatively high tracking gain must be used in order
to keep the bias error against a maneuvering target low. A comparison
was made of the responses obtained by using the high-gain system and the
low-gain system with integrator for three different initial conditions.

Figure 6 shows the calculated miss-distance responses for the high-
gain no-integration system for an initial radar lock-on angle of 7.5^O
against a nonmaneuvering and a maneuvering target, and for an initial
radar lock-on angle of 2^O against a maneuvering target. The abscissa
indicates time from lock-on. The early part of the motion is not shown
in order to obtain a reasonable scale factor for the final miss distances.
Each run ends at the firing time. For comparison, lines of constant
flight-path error of 20 mils are shown. Although the motions are oscil-
latory and have varying amounts of initial overshoot, the final miss
distance is small for each case, showing that the high-gain no-integrator
system can give satisfactorily low miss distances for a large variety
of initial conditions. It should be mentioned that against the maneuvering
target, an increment of 36 feet per g should be added to the calculated
final miss because of the curvature of the target flight path during the
time of flight of the rockets, which was assumed to be 1.5 seconds. The
oscillatory properties of the response were primarily caused by the
0.6-second time constant of the filter and the high tracking gain neces-
sary against a maneuvering target. Cutting this time constant in half
removed most of the undesirable oscillation. For lower tracking gain,
excellent no-overshoot responses could be obtained against a nonmaneu-
vering target even with the 0.6-second filter, but large bias errors
were obtained against the maneuvering target.

Figure 7 shows the miss distances, for the same set of initial con-
ditions, obtained by use of the tracking integrator with low tracking
gain. The amount of integrator gain was chosen to give an excellent
response for the initial 7.5^O radar angle against a maneuvering target.

This amount of integrator signal caused a large overshoot against the nonmaneuvering target and resulted in a final miss distance of about 200 feet. On the other hand, for the case of the small initial error against a maneuvering target, the integrator signal was too small and resulted in a miss distance of approximately 100 feet. These results illustrate a basic difficulty in the use of a constant-gain tracking integrator for a variety of lock-on angles and target maneuvers. Since the integrator signal must provide the bias command to build up a steady acceleration fairly rapidly even for small initial errors, it tends to cause large overshoots for large initial errors against a nonmaneuvering target. It would therefore seem that, if a tracking integrator is to be used, it would be desirable to have a nonlinear gain or, possibly, some device which would switch the integrator on only in the range of small errors. In the complete investigation, the high-gain system was used without the integrator.

Although there was not sufficient time for a detailed study of the autopilots on the Typhoon simulator, the gains chosen on the basis of the simplified studies appeared satisfactory. The effects of varying several of the most important gains were investigated, and in no case was it found desirable to change the gains predicted from the simplified analyses.

II - SOME RESULTS OF A STUDY PERFORMED ON THE TYPHOON COMPUTER

As pointed out in part I of this paper this study of the attack phase of the automatically controlled interceptor was performed on the Typhoon Computer. The purpose of this section is to present some of the results of the first phase of the investigation of the attack problem. The objectives of this phase were:

(1) To determine the necessary mathematical representation of the airplane for use in a simulation problem. This determination was made by studying the effect of the cross-coupling terms in the equations of motion.

(2) To study the effect of nonlinear aerodynamics on the airplane response.

Figure 8 shows the attack phase as set up for this study. The radar, computer, and flight-data instruments which supply interceptor flight data to the computer and automatic pilots were assumed to be dynamically perfect. The automatic pilot used in this study was described in section I of this paper.

The target was programed to fly a straight-line course at a Mach number of 1.4 at 50,000 feet or to perform a ±2g vertical-plane maneuver

at the same Mach number. The radar was assumed to be an automatic-tracking fire-control radar with a space-stabilized line of sight. The radar supplies the antenna angles, angular velocity of the line of sight, range, and range rate to the guidance computer. The computer, which in conjunction with radar forms a director type of fire-control system, uses the data supplied by the radar and α and β from the flight data sensors to solve the equations for a lead-collision rocket-firing course. The rocket is assumed to have an average flight velocity of 2,000 feet per second relative to the interceptor and a time of flight of 1.5 seconds.

The solution of the fire-control equations is presented as the predicted azimuth and elevation miss distances. The miss distances are then filtered, corrected for cross-roll effects and converted to azimuth and elevation steering errors ϵ_a and ϵ_e by the following formulas:

Azimuth steering error:

$$\epsilon_a = \frac{M_a}{R_f} \tag{1}$$

Elevation steering error and pitch command:

$$\epsilon_e = \frac{M_e}{R_f} \tag{2}$$

Roll command:

$$\epsilon_\phi = \tan^{-1}\frac{\epsilon_a}{\epsilon_e}$$

$$= \tan^{-1}\frac{M_a}{M_e} \tag{3}$$

The airplane equations of motion are expressed as follows:

$$m\left(\dot{u} + qw_o\right) + \left[m(\dot{q}\ \Delta w - rv)\right] = Wl_3 + F_X \tag{4}$$

$$m(\dot{v} + ru_0 - pw_0) + \left[m(r\,\Delta u - p\,\Delta w)\right] = Wm_3 + F_Y \qquad (5)$$

$$m(\dot{w} - qu_0) + \left[m(pv - q\,\Delta u)\right] = Wn_3 + F_Z \qquad (6)$$

$$I_X\dot{p} + \left[\left(I_Z - I_Y\right)qr\right] = L' \qquad (7)$$

$$I_Y\dot{q} + \left[\left(I_X - I_Z\right)pr\right] = M' \qquad (8)$$

$$I_Z\dot{r} + \left[\left(I_Y - I_X\right)pq\right] = N \qquad (9)$$

$$\dot{l}_1 = m_1 r - n_1 q \qquad (10)$$

$$\dot{m}_1 = n_1 p - l_1 r \qquad (11)$$

$$\dot{n}_1 = l_1 q - m_1 r \qquad (12)$$

$$i = 1,\ 2,\ 3 \qquad (13)$$

Equations (4) to (9) are six-degree-of-freedom rigid-body equations of
motion referenced to principal body axes and are referred to herein as
"complete" equations. The equations of motion were analogued so that
the cross-coupling terms, which are the terms in brackets in equations (4)
to (9), could be deleted. When these terms are deleted the equations
reduce to a set of linear equations which approximate the classical linear
airplane stability equations.

The direction cosines, obtained from the equations (11) to (13), are used to supply interceptor attitude information needed to simulate the radar. The direction cosines l_3, m_3, and n_3 were used to account accurately for gravity accelerations in the force equations.

The aerodynamics considered for the problem include nonlinearities in the stability derivatives that were functions of the Mach number and angle of attack. The derivatives $C_{n_{\dot{\beta}}}$ and $C_{l_{\dot{\beta}}}$ were omitted, as were the aerodynamic cross-coupling terms such as C_{m_β}.

The first objective, which was to study the airplane representation, was carried out by making computer runs with the complete and linear equations of motion. Some of these results are shown in figure 9. The diagram at the right shows the initial condition used. The target and interceptor are flying at right angles to each other and the line of sight at lock-on is displaced 45° in azimuth from the center line of the interceptor. The lock-on range along the line of sight is 60,000 feet and the interceptor flight condition is straight and level trimmed flight at a Mach number of 2.2. The time histories show bank angle and normal acceleration, for 18 seconds, from time of lock-on to the firing point.

The differences between the results obtained with the complete equations and with the linear equations are errors introduced when a linear representation of the airplane is assumed. Similar errors occurred in the other degrees of freedom of the airplane and for other bow and beam attacks with different initial conditions. By systematic deletion of the cross-product terms in the equations of motion, these errors were traced to the omission of cross-coupling terms that are functions of rolling velocity. Of these terms, $p \, \Delta w$ in the side-force equation (5) was found to be the dominant term. The other cross-coupling terms involving rolling velocity, pv, pq, and pr, while producing smaller effects than $p \, \Delta w$, cannot be neglected. The cross-coupling terms such as rv and qr had no apparent effect on the airplane response.

Figure 10 shows the predicted terminal miss distances as obtained for the complete and linear representations of the airplane. The use of the linear equations introduces errors in the predicted terminal miss distances of approximately 300 feet in azimuth and 500 feet in elevation.

As discussed in the first section the airplane response becomes oscillatory when the limit on the rate of control-surface deflection is reduced. The results of this study indicate that, when the airplane is represented by complete equations, lower control-surface rate limits can be used before the airplane response becomes oscillatory. Thus, for the system considered the critical rate of control-surface deflection should be determined when the airplane is represented by the complete equations.

The linear equations with the rolling-velocity cross-product terms added were used to represent the airplane and reductions in the rate of control-surface deflection gave results that were the same as for the complete equations.

The results of the investigation of the representation of the airplane may be summarized as follows: The use of linear equations to represent the airplane introduces errors in the airplane response and the azimuth and elevation miss distances. In addition the use of linear equations predicts a high value for the critical rate of control-surface deflection. These differences were found to be functions of the cross-product terms that involve rolling velocity. Thus for the airplane and guidance system considered the airplane can be represented by the linear equations with $p \Delta w$, pv, pq, and pr added.

The second objective of the calculations made on the Typhoon Computer was to study the effects of nonlinear aerodynamic parameters on the airplane response. The results of wind-tunnel tests were used to obtain representative nonlinear aerodynamics for incorporation in the problem. The nonlinear aerodynamic parameters were programed as polynomial functions of the Mach number and angle of attack. Figure 11 shows the variations in pitching-moment coefficient C_m and the stability derivatives C_{n_β} and C_{l_β} with Mach number and angle of attack. The linear values of C_m and C_{n_β} are obtained by extending the straight line that runs from $\alpha = 0^\circ$ to $\alpha = 6^\circ$ through the angle-of-attack range. In the case of C_{l_β} the value corresponding to the trim angle of attack ($\alpha = 2^\circ$) was used. In figure 11 the nonlinear part of the airplane parameters shown starts at $\alpha = 6^\circ$. Provisions were made for the angle of attack at which the nonlinearity started to be varied. In addition to the stability derivatives shown in figure 11, C_{l_p} and C_{n_p} were programed with nonlinear variations.

Calculations were made with the nonlinear pitching-moment coefficient added to the airplane representation. In figure 12 are presented time histories of normal acceleration and elevator deflection obtained by use of the linear and nonlinear values of C_m. The time histories in this figure show that part of an 18-second attack run during which the nonlinear portion of C_m was effective. Although the curves for normal acceleration show differences, the integrals of the normal acceleration over the time interval during which the nonlinear C_m is effective are approximately equal. The largest differences occurred in elevator deflection. A comparison of the elevator deflections for the linear and nonlinear pitching-moment coefficients shows that the elevator deflections are the same for the first part of the time history but that large differences occur in the last part of the time history for the same normal

acceleration. These results indicate that the automatic pilot was able to cope with the changes in aerodynamics and to maintain the same normal acceleration by moving the control surface in a different manner.

Figure 13 shows time histories of the rolling-velocity response and aileron deflection for linear and nonlinear lateral stability derivatives. The rolling-velocity response was the same for the linear and nonlinear derivatives. The aileron deflection for this rolling-velocity response with linear derivatives is shown by the solid line in the lower set of curves. When the nonlinear C_{n_β} was added, in a manner to decrease the directional stability as the angle of attack increased, large sideslip velocities developed. The contribution of $C_{l_\beta}\beta$ to the rolling moment increases and tends to counter the rolling velocity and, as shown by the dash-line curve, more aileron deflection is required to maintain the same rolling velocity. When the nonlinear C_{l_β} was added in a manner to reduce the positive effective dihedral with angle of attack, the $C_{l_\beta}\beta$ effect decreased and the aileron motion followed the curve labeled "nonlinear $C_{n_\beta} + C_{l_\beta}$". The aileron deflection required to maintain the rolling response when all nonlinear derivatives were present is also shown in this figure. As was found in the study of pitching moments, the automatic pilot copes with the changes in aerodynamics and makes use of different control-surface deflections to compensate for this change and thereby maintains the same rolling velocity when the nonlinear aerodynamic parameters are used.

These results indicate that, for the interceptor system considered, nonlinearities in the airplane stability derivatives do not affect the airplane response in pitch or in roll. However, different control-surface motions are required to maintain the airplane response. Thus, if nonlinearities exist in the airplane stability derivatives, these nonlinearities should be included as part of the airplane simulation in order to obtain realistic control-surface deflections.

In addition to the two primary objectives of this study some problems associated with the roll command were investigated.

The vertical-plane studies of the interceptor problem reported in part I of this paper (figs. 6 and 7) showed that a high-gain longitudinal control system was required to track a maneuvering target when integrators were omitted from the tracking loop. The high-gain longitudinal control system was used in this study. In addition, these results indicated that changes in sign of the elevation steering error will occur. These changes in sign of the elevation steering error have a detrimental effect on the roll-control system because of the type of roll command used thus far in this study. For this reason, the high-gain longitudinal

control system was studied with three different roll commands, which are
illustrated in figure 14.

These sketches are a presentation of the guidance computer output.
The axes of the computer are coincident with the interceptor reference
axes and the predicted impact point may appear at any point in the plane.
The predicted impact point is displaced from the origin by the steering
errors ϵ_a positive along the interceptor Y-axis and ϵ_e positive along
the interceptor negative Z-axis. When the type I roll command (the roll
command used up to now) is used and the predicted impact point is in the
first quadrant, the interceptor rolls to the right through angle ϵ_ϕ and
uses positive acceleration to reduce the steering errors to zero. If ϵ_e
changes sign during the attack run, a large aileron kick is commanded as
ϵ_e passes through zero. The type II roll command illustrated in fig-
ure 14 eliminates this large aileron kick by switching the roll command
from the inverse tangent to one that is proportional to azimuth steering
error. This switch occurs when the predicted impact point appears within
the circular boundary ϵ_{cr} (that is, $\epsilon < \epsilon_{cr}$). Another difficulty is
associated with both the type I and type II roll commands. This problem
is illustrated in the third sketch in figure 14. When the impact point
appears at the point labeled (1) in the diagram, the interceptor is ordered
to roll through the angle ϵ_{ϕ_1}, which is greater than 90°. Since the sign
of ϵ_e is negative, the interceptor develops a negative acceleration and,
under this influence, moves down and away from the target until the roll
has changed the sign of ϵ_e. One way to alleviate this condition is to
change the roll order when ϵ_e is negative so that the predicted impact
point appears as though it were located at point (2) in the diagram.
When this change is made, the interceptor rolls to the left through the
small angle ϵ_{ϕ_2} to reduce the azimuth miss distance to zero. However,
the command to the longitudinal control system, ϵ_e, is unchanged and the
interceptor uses negative acceleration to close on the correct impact
point located at (1). The type III roll command is the same as the type II
command, except that such a change has been made for $|\epsilon| < \epsilon_{cr}$. In this
case the only change needed is to reverse the sign of the roll order when
$\epsilon_e < 0$. Thus, the interceptor will roll through the smallest angle to
provide zero azimuth miss distance.

Figure 15 compares the rolling-velocity response and aileron deflec-
tions for these three roll commands. In this case the interceptor is
making a head-on attack against a nonmaneuvering target. Again the lock-
on range is 60,000 feet and the Mach numbers of the interceptor and target
are 2.2 and 1.4, respectively.

A comparison of the type I command with the type II command shows that the type II command tends to reduce the large aileron kicks and rolling velocities that occur when the type I command is used as ϵ_e passes through zero. A comparison of the type III roll-command response with the responses for the other two roll commands indicates that the type III roll command eliminates the difficulties experienced with the other two roll commands. An examination of the normal-acceleration response showed it to be less oscillatory and from 4.25 seconds the interceptor used negative acceleration to close on the predicted impact point. The peak normal acceleration during this part of the run was -2g.

A complete evaluation of the type III roll command could not be made, inasmuch as the interceptor assumed an inverted attitude for the last part of the attack run. This result was probably caused by the lack of proper sequencing of the roll and flight-path commands and by the omission of gravity corrections from the roll order. The inverted flight attitude, consequently, is not believed to represent an inherent defect of the type III roll command.

One more point, the speed loss during the attack run, is worthy of mention. The speed loss was found to be a function of initial condition and ran as high as 12 percent of the initial velocity for attack runs against a nonmaneuvering target. Speed losses as high as 25 percent were observed when the target was making a 2g maneuver.

Langley Aeronautical Laboratory,
    National Advisory Committee for Aeronautics,
        Langley Field, Va., May 11, 1955.

REFERENCE

1. Schy, Albert A., and Gates, Ordway B., Jr.: Analysis of Effects of
      Airplane Characteristics and Autopilot Parameters on a Roll-Command
      System With Aileron Rate and Deflection Limiting. NACA RM L55E18,
      1955.

CONTROL–SYSTEM TIE-IN SIGNALS

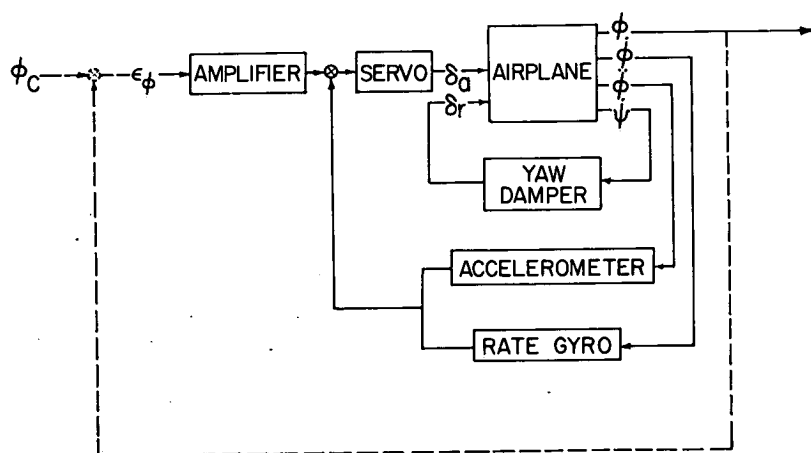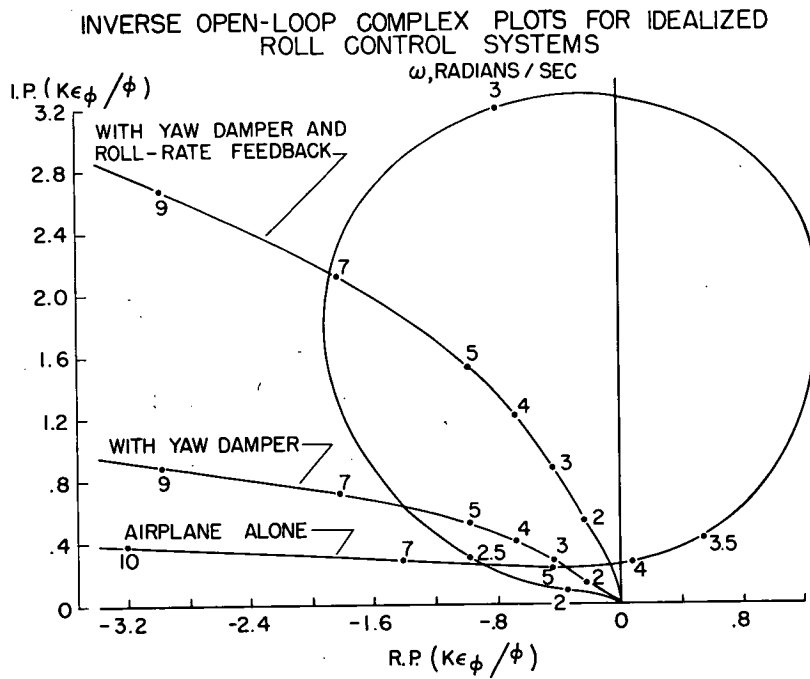LATERAL   LONGITUDINAL

$$\epsilon_\phi = \tan^{-1}(M_a/M_e)$$

$$\epsilon_e = \frac{M_e}{R_f} \approx (\Delta\gamma)_D$$
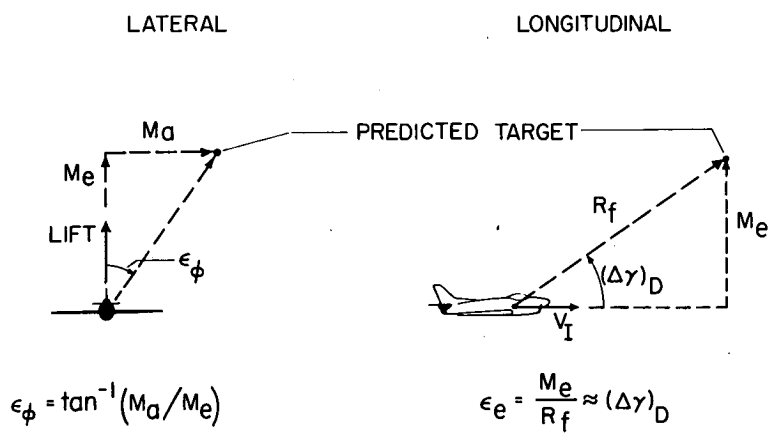
Figure 1

LATERAL CONTROL SYSTEM

Figure 2

INVERSE OPEN-LOOP COMPLEX PLOTS FOR IDEALIZED
ROLL CONTROL SYSTEMS

Figure 3

EFFECT OF ROLL-RATE AND ACCELERATION
FEEDBACKS ON RATE-LIMITING INSTABILITY
AILERON LIMITS: ±20° AND ±120°/SEC
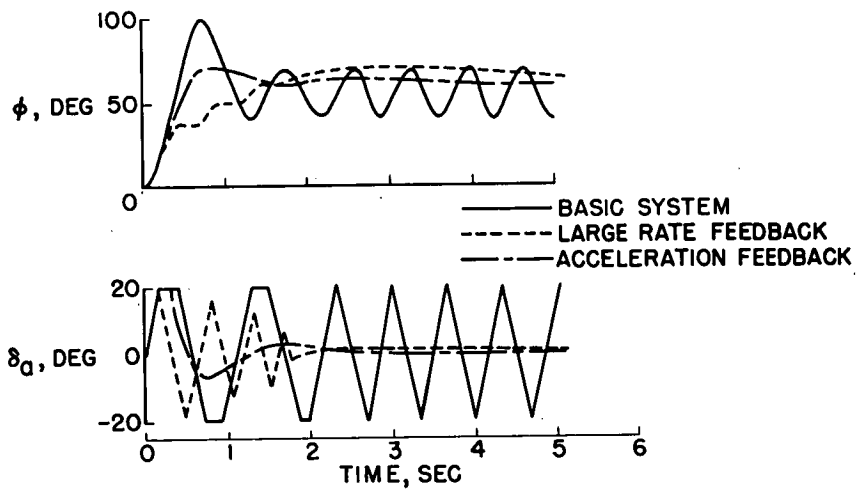
Figure 4

LONGITUDINAL CONTROL SYSTEM
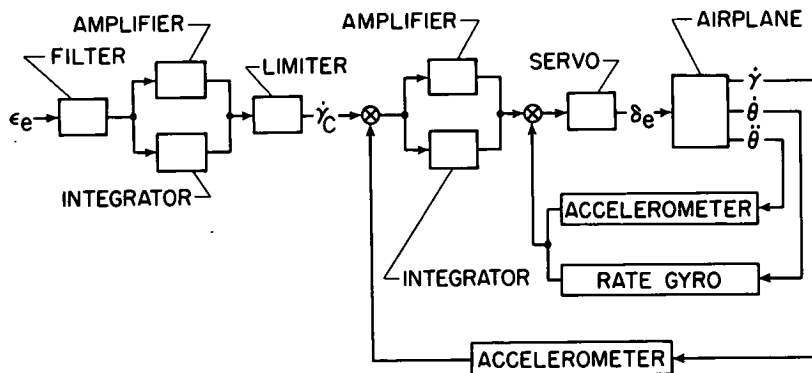
Figure 5

PREDICTED MISS AT FIRING TIME WITH HIGH TRACKING
GAIN AND NO TRACKING INTEGRAL

Figure 6

PREDICTED MISS AT FIRING TIME WITH LOW
TRACKING GAIN AND TRACKING INTEGRAL
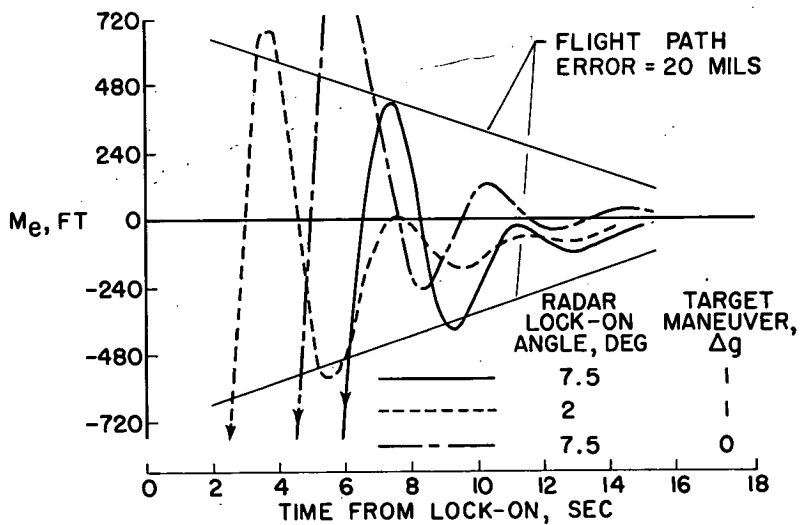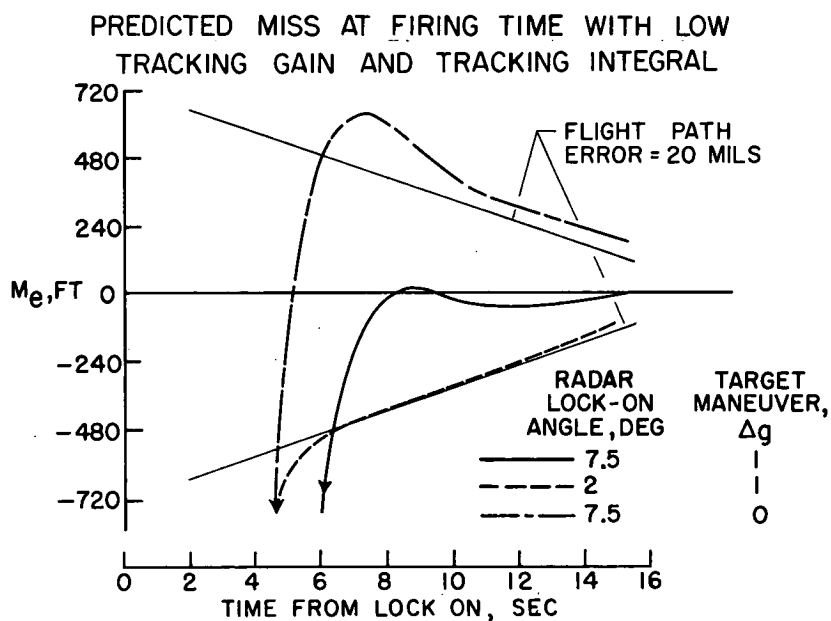
Figure 7

SCHEMATIC DIAGRAM OF INTERCEPTOR SYSTEM SHOWING
COMPONENTS AND DATA FLOW
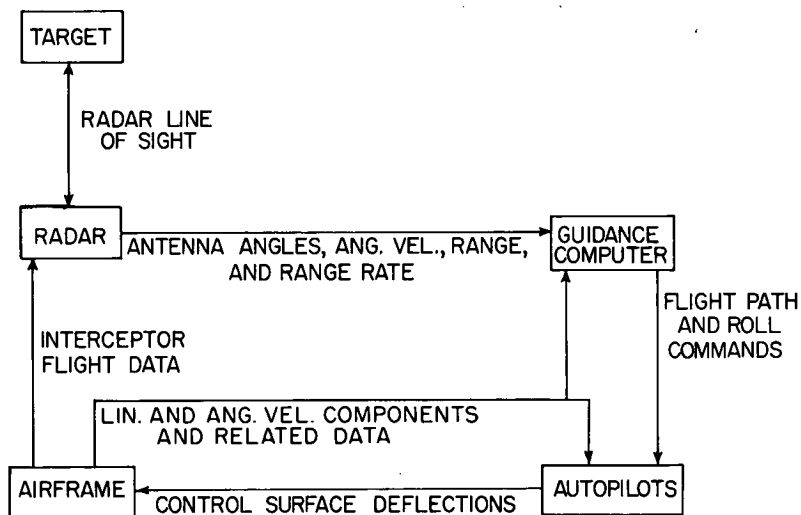
Figure 8

COMPARISON OF AIRPLANE RESPONSE FOR THE COMPLETE
AND LINEAR EQUATIONS
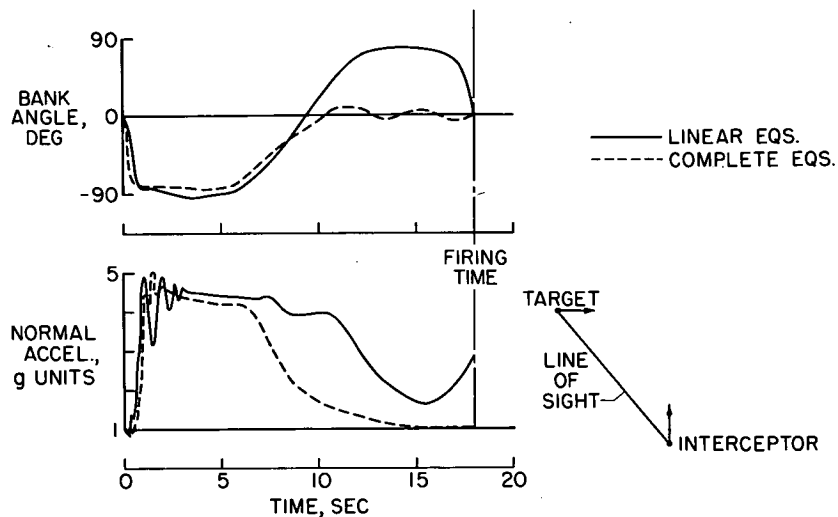
Figure 9

COMPARISON OF MISS DISTANCES FOR THE COMPLETE
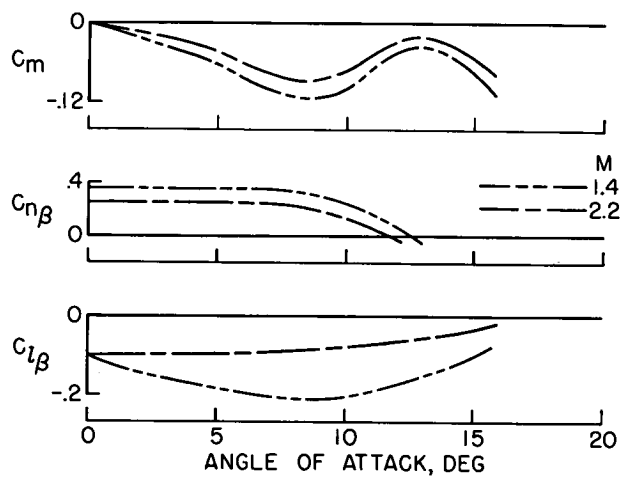AND LINEAR REPRESENTATIONS OF THE AIRPLANE
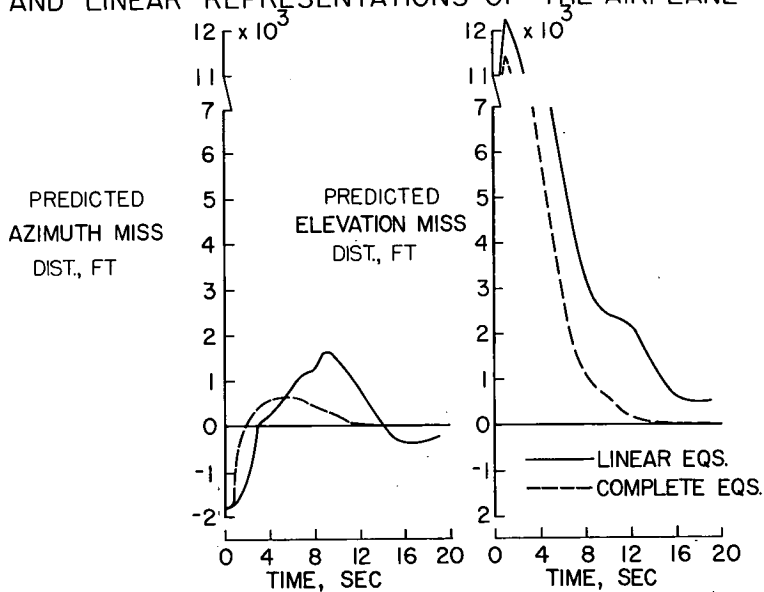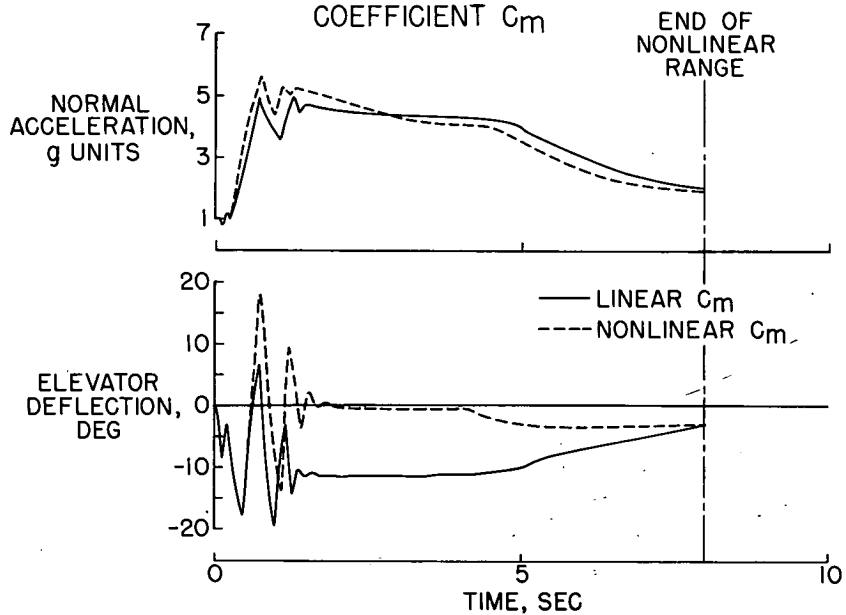

Figure 10

NONLINEAR AERODYNAMICS

Figure 11

NONLINEAR AERODYNAMICS – EFFECT OF PITCHING-MOMENT
COEFFICIENT C_m

Figure 12

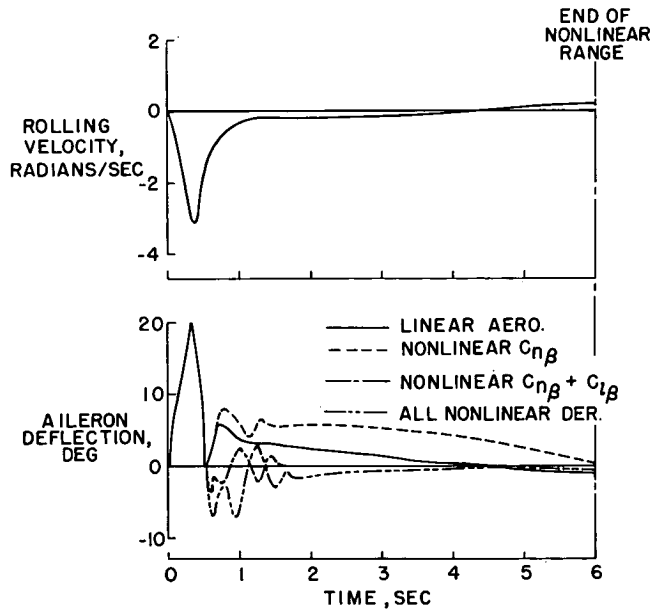NONLINEAR AERODYNAMICS - EFFECT ON LATERAL RESPONSE
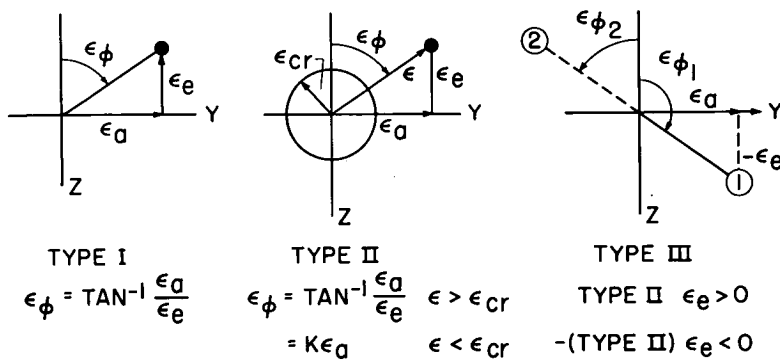
Figure 13
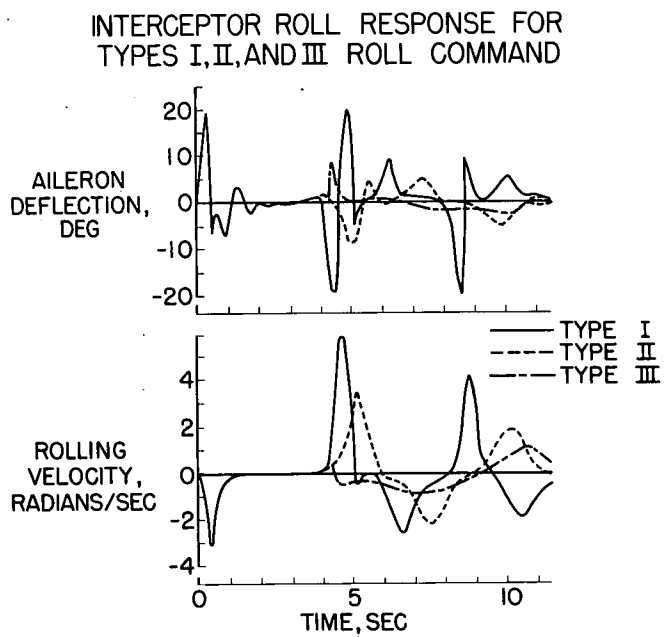
ROLL COMMAND VARIATIONS

Figure 14

INTERCEPTOR ROLL RESPONSE FOR
TYPES I, II, AND III ROLL COMMAND

AILERON
DEFLECTION,
DEG

ROLLING
VELOCITY,
RADIANS/SEC

TIME, SEC

—— TYPE I
---- TYPE II
—·— TYPE III

Figure 15